Corresponding Author: Professsor Chao-Ming Huang, Ph. D.

Corresponding Author's Institution: Kun Shan University

First Author: Chao-Ming Huang, Ph. D.

Order of Authors: Chao-Ming Huang, Ph. D.; Wen-Sheng Chang, Ph. D.; Yu-Chu M. Li, Ph. D.; Tsair-Wang Chung, Ph. D.; Yung-Sen Lin, Ph. D.

Suggested Reviewers: Takuya Suzuki
Department of Chemical Processes and Environments Faculty of Environmental Engin, Kitakyushu University
Suzuki-t@env.kitakyu-u.ac.jp
good at developing green materials for environmetal protection

Chiaki Yokoyama
Institute of Multidisciplinary Research for Advanced Materials, Tohoku University
chiaki@tagen.tohoku.ac.jp
good at synthesizing advanced materials

Akihiko Kudo
Department of Applied Chemistry Faculty of Science, Tokyo University of Science
a-kudo@rs.kagu.tus.ac.jp
good at synthesizing visible-light-driven photocatalysts

Professor W. Ueda

Catalysis Research Center, Hokkaido University, Kita21-Nishi10, Kita-Ku, 001-0021

Sapporo, Japan, Email: ueda@cat.hokudai.ac.jp

Dear Prof. W. Ueda:

We would like to submit the manuscript entitled "Toluene decomposition using silver vanadate/SBA-15 photocatalysts: DRIFTS study of reaction intermediates and regeneration", which we wish to be considered for publication in Applied Catalysis A: General.

We believe that two aspects of this manuscript will make it interesting to general readers of Applied Catalysis A: General. First, we reported that silver vanadate/SBA-15 photocatalysts was successfully prepared by incipient wetness impregnation method. Second, we show that the abundant surface hydroxyl groups and high intensities of Brønsted and Lewis acids on the SVO/SBA-15 composites are considered the main causes of the enhanced adsorption capacity, outstanding photoactivity, and long term stability in the photodegradation of toluene. Our findings may have important applications in elimination of environment pollutants.

Sincerely Yours,

Dr. Chao-Ming Huang

Professor

Department of Environmental Engineering

Kun Shan University, Tainan, Taiwan

Applied Catalysis A: General

Toluene decomposition using silver vanadate/SBA-15 photocatalysts: DRIFTS study of reaction intermediates and regeneration

Dear editor,

Thank you for your useful comments and suggestions on the structure of our manuscript. We have modified the manuscript accordingly, and the detailed corrections are listed below point by point:

Comments:

1) Each point provided in the research highlights should not exceed 85 characters including spaces.

√ The research highlights did not exceed 85 characters including spaces. The detailed highlights are as follows:

➢ SVO/SBA-15 composite was synthesized using a wetness impregnation procedure.

➢ SVO/SBA-15 has a much higher photodegradation ability than those of P25 and SVO.

➢ The DRIFT spectra prove the main oxidation intermediate of toluene is benzaldehyde.

➢ Surface OH, Brønsted, and Lewis acids are responsible for photoactivity.

The manuscript has been resubmitted to your journal. We look forward to your positive response.

Sincerely,

Dr. Chao-Ming Huang

Professor

Department of Environmental Engineering

Kun Shan University

Toluene decomposition using silver vanadate/SBA-15 photocatalysts: DRIFTS study of reaction intermediates and regeneration

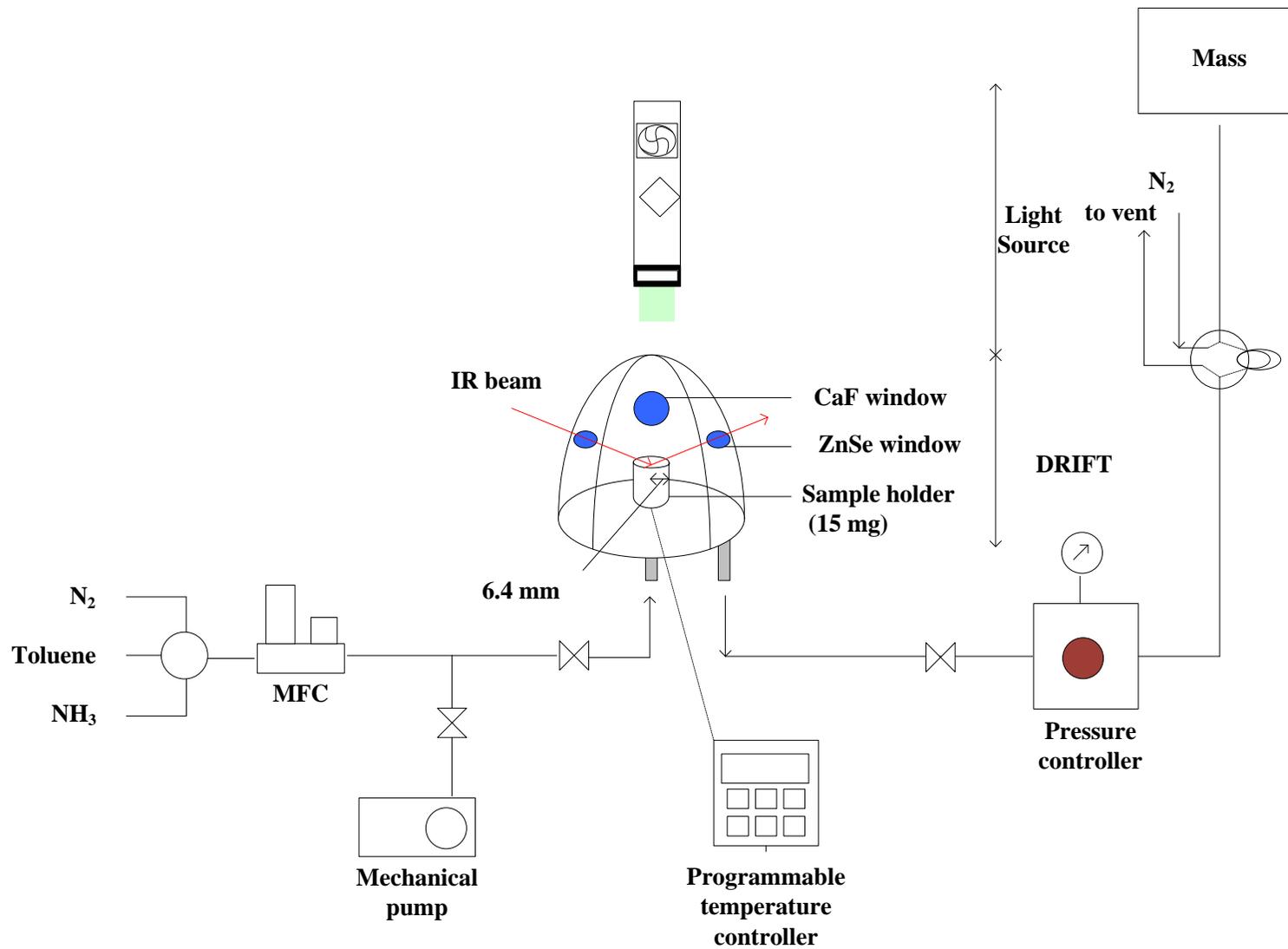Wen-Sheng Chang[a], Yu-Chu M. Li[b], Tsair-Wang Chung[c], Yung-Sen Lin[d], Chao-Ming Huang[e,*]

[a]*Green Energy & Environment Research Labs, Industrial Technology Research Institute, Hsinchu, Taiwan*

[b]*Department of Mechanical Engineering, Southern Taiwan University, Tainan, Taiwan*

[c]*Department of Chemical Engineering/R&D Center for Membrane Technology, Chung Yuan Christian University, Taoyuan, Taiwan*

[d]*Department of Chemical Engineering, Feng Chia University, Taichung, Taiwan*

[e]*Department of Environmental Engineering, Kun Shan University, Tainan, Taiwan*

DRIFTS is one of the most frequently used tools for simultaneously obtaining information concerning the reaction and the characteristics of the catalyst surface.

Research highlights

➢ SVO/SBA-15 composite was synthesized using a wetness impregnation procedure.

➢ SVO/SBA-15 has a much higher photodegradation ability than those of P25 and SVO.

➢ The DRIFT spectra prove the main oxidation intermediate of toluene is benzaldehyde.

➢ Surface OH, Brønsted, and Lewis acids are responsible for photoactivity.

Toluene decomposition using silver vanadate/SBA-15 photocatalysts:

DRIFTS study of reaction intermediates and regeneration

Wen-Sheng Chang[a], Yu-Chu M. Li[b], Tsair-Wang Chung[c], Yung-Sen Lin[d], Chao-Ming

Huang[e,]*

[a]*Green Energy & Environment Research Labs, Industrial Technology Research Institute,*

Hsinchu, Taiwan

[b]*Department of Mechanical Engineering, Southern Taiwan University, Tainan, Taiwan*

[c]*Department of Chemical Engineering/R&D Center for Membrane Technology, Chung*

Yuan Christian University, Taoyuan, Taiwan

[d]*Department of Chemical Engineering, Feng Chia University, Taichung, Taiwan*

[e]*Department of Environmental Engineering, Kun Shan University, Tainan, Taiwan*

*Corresponding author. Tel: +886-6-2050359; Fax: +886-6-2050540

E-mail address: charming@mail.ksu.edu.tw (C.M. Huang)

Address: 949 Da-Wan Rd. Yung-Kang Dist., Tainan 71003, Taiwan

Abstract

Silver vanadate (SVO) containing SBA-15 visible-light-driven photocatalyst was synthesized using the incipient wetness impregnation procedure. The formation of reaction intermediates during the photocatalytic oxidation of gaseous toluene and the reliability test of SVO/SBA-15 were characterized by in situ diffuse reflectance infrared Fourier transform spectroscopy (DRIFTS). The SVO/SBA-15 photocatalyst has a much higher photodegradation ability than those of P25 (nano-TiO$_2$) and plain SVO. The sample loaded with 51 wt% SVO (51SVO/SBA-15) exhibited the best photocatalytic activity. The DRIFT spectra indicate that the main oxidation intermediate of toluene is benzaldehyde. The results of two consecutive cyclic runs and regeneration indicate that the accumulation of benzaldehyde causes an irreversible deactivation of P25, but no deactivation of 51SVO/SBA-15. DRIFTS also confirms the presence of surface hydroxyl groups and Brønsted and Lewis acids on the SVO/SBA-15 composites. The abundant surface hydroxyl groups and high intensities of Brønsted and Lewis acids are considered the main causes of the enhanced adsorption capacity, outstanding photoactivity, and long term stability of the SVO/SBA-15 composites.

Keywords: SBA-15; Visible-light-driven photocatalyst; Toluene photo-oxidation; Surface hydroxyl groups

1. Introduction

Volatile organic compounds (VOCs), extensively used as solvents, aerosol propellants, and raw materials, are considered as great contributors to atmospheric pollution, with some considered toxic. Due to increasing eco-awareness, regulations set by governments regarding the emission of VOCs have grown stricter. The most conventional reduction method of VOCs is adsorption technology, which transforms air pollutants into another phase, creating secondary pollution. Since the adsorption of VOCs does not actually destroy the pollutants, the regeneration of adsorbents is a problem after saturation. Among the available alternatives to adsorption, photocatalytic oxidation (PCO) is quite promising for VOC reduction as it has the potential to completely mineralize VOCs to CO_2 and H_2O, which may meet the requirements of more stringent VOC emission control in the future. A vast number of studies related to titanium dioxide, a UV-active photocatalyst, have been conducted. Recently, a lot of research effort has been devoted to loading TiO_2 species onto or incorporating them into the mesoporous silica called Santa Barbara Amorphous-15 (SBA-15) to combine adsorption and photocatalysis for the rapid removal of VOCs [1-4]. However, the use of titania-SBA-15 composites is hindered by some major shortcomings. First, TiO_2 has low efficiency of degrading VOCs under visible light illumination due to its wide band gap, which is in the range of 3.0-3.2 eV. Second, the most general method for

synthesizing TiO$_2$ is the sol–gel method, which requires high-temperature calcination (673 K or higher) to obtain good crystallinity. Moreover, the reaction intermediates can be in some cases more toxic and/or stable than the parent VOC during the PCO process. Therefore, the development of visible-light-active photocatalysts that can minimize the amount of intermediates during the photocatalytic process is desirable.

The present work demonstrates the preparation of silver vanadate/SBA-15 composites (SVO/SBA-15) via hydrothermal synthesis using a post-synthesis step without high-temperature calcination. The photodecomposition of toluene was selected as a model reaction because toluene is a common atmospheric indoor and industrial air pollutant. In situ diffuse reflectance infrared Fourier transform spectroscopy (DRIFTS), one of the most frequently used tools for simultaneously obtaining information on species and the characteristics of the catalyst surface during a reaction, was used to monitor the reaction intermediates. Toluene has usually shown high initial conversions followed by very low steady-state conversions, which has been attributed to catalyst deactivation during the PCO process [5]. In order to determine the stability of the SVO/SBA-15 composites, the reliability test of the SVO/SBA-15 composites was investigated using Fourier transform infrared (FTIR) spectroscopy.

2. Experimental Procedure

2.1. Preparation of photocatalyst

4

SBA-15 was synthesized with Pluronic P123 ($EO_{20}PO_{70}EO_{20}$, M_{av} = 5800; Aldrich) and tetraethylorthosilicate (TEOS) according to a previous report [6]. Briefly, 4.0 g of P123 was dissolved in 30 g of de-ionized water and 120.0 g of HCl solution (2 M) with stirring at 313 K for 2 h. Then, 8.5 g of TEOS was added into the P123 solution, which was stirred for another 22 h until a white gel precipitated. The gel was transferred to a Teflon bottle and heated at 403 K for 24 h. The precipitate was filtered, washed several times with de-ionized water, dried overnight at 373 K, and then calcined at 773 K (heating rate of 1 K/min) for 4 h in air.

The silver-vanadate-loaded SBA-15 (SVO/SBA-15) was prepared via the incipient wetness impregnation procedure. In the preparation process, 0.204 g $AgNO_3$ was dissolved in urea aqueous solution (120 g H_2O, 0.577 g urea) with stirring at room temperature for 0.5 h to obtain solution A. Solution B was prepared by mixing 0.047 g NH_4VO_3 with 0.3 g SBA-15 in de-ionized water at 343 K for 1 h under an ultrasonic bath. A suspension formed when solution A was added dropwise to solution B under vigorous stirring for 1 h. The molar composition of the suspension $AgNO_3/NH_4VO_3/CO(NH_2)_2$ was 3.0/1.0/12.0. The suspension was titrated to pH 7 using ammonia solution, followed by additional stirring at room temperature for 24 h. Finally, the as-obtained suspension was transferred into a Teflon-lined autoclave with hydrothermal treatment (temperature: 413 K, time: 4 h). After the hydrothermal

procedure, the resulting precipitates were collected and washed with de-ionized water three times, and then dried at 353 K for 12 h. These samples were denoted xSVO/SBA-15, where x represents the weight percentage of silver vanadate (wt%). The sample synthesized under identical conditions without the addition of SBA-15 was denoted SVO.

2.2. Sample characterization

The X-ray diffraction (XRD) patterns of the powders were measured using an X-ray diffractometer (PANalytical X'Pert PRO) with Cu radiation ($\lambda = 0.15418$ nm) in the 2θ range of 20 to 60°. High-resolution transmission electron microscopy (HRTEM) images of the samples were observed on a Philips Tecnai G2 F20 microscope equipped with energy-dispersive X-ray spectroscopy (EDX) operated at an accelerating voltage of 200 kV. Photoluminescence (PL) spectra were recorded by a fluorescence spectrophotometer (Dongwoo Optron) under excitation at 325 nm. In situ DRIFTS measurements were performed using a PerkinElmer FTIR spectrometer (Spectrum GX) and a diffuse reflectance accessory (Harrick Scientific, DRP-PE9) with a temperature- and atmosphere-controlled high-temperature low-pressure reaction cell (Harrick Scientific, HVC-DRP-3). Prior to the IR measurements, the samples were dehydrated under vacuum from room temperature to 523 K at 10 K min^{-1} in N$_2$ flow (30 ml min^{-1}), held at 523 K for 30 min, and then cooled to 303 K. DRIFT spectra with a resolution of

4 cm^{-1} were collected in the interval of 2800-4000 cm^{-1} for surface hydroxyl functional

groups [7]. Ultraviolet-visible (UV-Vis) spectra were collected by a spectrophotometer

(JASCO V-500) equipped with an integrating sphere assembly over the range of 400 to

700 nm. The surface area and pore volume of the as-prepared samples were determined

using a volumetric sorption analyzer (Micromeritics ASAP 2020). The samples were

degassed at 473 K under vacuum conditions for a period of at least 4 h prior to

measurements. The nitrogen adsorption/desorption isotherms were measured over a

relative pressure (P/P_0) range of approximately 10^{-3} to 0.995. The surface areas were

calculated using the Brunauer-Emmett-Teller (BET) method in the relative pressure

range of 0.06-0.2. The pore size distributions were determined from the analysis of the

adsorption isotherm using the Barret–Joyner–Halenda (BJH) algorithm. The total pore

volumes were estimated from the adsorbed N$_2$ amount at $P/P_0 = 0.973$.

2.3. Photocatalytic activity evaluation with MS and DRIFTS

The photocatalytic oxidation of toluene was performed in situ in an IR cell with

ZnSe windows. An LED lamp, with a wavelength ranging from 430 to 620 nm with a

photon intensity of 4 mW/cm^2, was used as the visible-light source [8]. A gaseous

toluene/N$_2$ mixture was generated, corresponding to the target toluene concentration of

200 ppmv. Prior to the experiments, the samples were pre-treated by heating and

flushing with N$_2$ flow (20 ml/min) from room temperature to 523 K, held at 523 K for

30 min, and then cooled to 303 K. The procedure for all PCO experiments was as follows: (1) toluene/N_2 flow was introduced into the photoreactor at a constant flow rate of 20 ml/min; (2) when the photoreactor inlet and outlet toluene concentrations were approximately equal, the LED lamp was turned on and the toluene/N_2 flow was stopped; (3) the photoreactor was flushed with the N_2 flow at 5 ml/min for 30 min, and then the N_2 flow was stopped. To verify the gaseous products (intermediates), the samples were monitored on-line with a quadrupole mass spectrometer (MS, SRS QMS300) at regular intervals. The spectra of the adsorbed species on the catalyst surface were recorded under both darkness and illumination. The spectra of the catalyst and the reaction intermediates during the reaction were expressed in units of Kubelka-Munk (K-M).

2.4. DRIFT characterization of NH_3 species

To determine the types of acid site present on the samples, temperature-programmed desorption of ammonia (NH_3) was carried out using DRIFT. Ammonia usually provides the probe molecules in spectroscopic experiments to determine the type of acid site in heterogeneous catalysis: Brønsted sites or Lewis sites. Prior to the experiments, the samples were heated in situ from room temperature to 523 K at 10 K/min in N_2 flow (30 ml/min), held at 523 K for 30 min, and then cooled down to 303 K. The samples were saturated at 303 K with a gas mixture of 5% NH_3 in N_2 (30 ml/min) for 30 min. At the end of the saturation process, the samples were flushed with

N_2 flow (30 ml/min). Then, the samples were heated again at a heating rate of 10 K/min from 30 K to 523 K and held at 523 K for 60 min. The DRIFT spectra with a resolution of 4 cm^{-1} were collected in the interval of 1200-1700 cm^{-1} for determining surface acidity.

3. Results and discussion

3.1. X-ray diffraction analysis

The XRD patterns of SVO and SVO-SBA-15 are shown in Fig. 1. Fig. 1a shows the low-angle XRD patterns of SBA-15 and SVO/SBA-15 samples. The XRD pattern of SBA-15 shows three well resolved peaks: a sharp peak at 1.0° and two weak peaks near 1.5 and 2.0°, respectively, which can be indexed to (100), (110), and (200) reflections of an ordered hexagonal *P6mm* space group, respectively. For SVO/SBA-15 samples, the XRD peaks decreased in intensity, which was probably caused by the decreasing scatter contrast between pore walls and the pore space with the introduction of SVO. For the samples with high SVO content, the intensities of the peaks are much weaker but can still be discerned, demonstrating that the uniform porous structure of SBA-15 is retained. The unit-cell parameter (a_0) of SVO/SBA-15 catalysts (ca. 13.0-14.0 nm) is larger than that of SVO (11.8 nm). This may be ascribed to the partial incorporation of SVO into the framework of SBA-15. Fig. 1b shows wide-angle XRD patterns of three SVO/SBA-15 samples and SVO. As can be seen, the SVO/SBA-15 composites had

pure α-Ag$_3$VO$_4$ (JCPDS card no. 43-0542). The crystalline structure of the bulk SVO was the same as that of the SVO/SBA-15 samples.

3.2. Porosity and surface area characterization

Fig. 2 shows the nitrogen adsorption-desorption isotherms of SBA-15 and SVO/SBA-15 samples. The N$_2$ adsorption-desorption isotherms of SBA-15 show type IV adsorption with a H1 hysteresis loop, indicating a mesoporous characteristic. For the SVO/SBA-15 samples, a sharp inflection in the relative pressure (*P/P$_0$*) range of 0.65 to 0.95, corresponding to capillary condensation within uniform mesopores, was observed. Compared to SBA-15, the capillary condensation of SVO/SBA-15 shifted to higher relative pressure, indicating an increase of the pore diameter when SVO was loaded into/onto SBA-15. The textural properties of SBA-15 support and SVO/SBA-15 samples are listed in Table 1. It can be seen that the specific surface area and pore volumes of SVO/SBA-15 samples significantly decrease with increasing silver vanadate loading, whereas the pore diameter increases. When the SVO/SBA-15 samples were synthesized using a post-synthesis method, the silver and vanadate species reacted on the surface of SBA-15; thus, the BET surface and pore volumes of SVO/SBA-15 composites decreased with increasing amount of SVO. The average pore diameter increased for SVO/SBA-15, which might be due to the small pores of SBA-15 being obstructed by silver vanadate nanoparticles.

3.3. Morphology

To better understand the formation of SVO nanocrystals on the mesopores and explore the effect of SVO on the pore structure of SVO/SBA-15 photocatalyst, HRTEM images were recorded. HRTEM images of SBA-15 and 51SVO/SBA-15 samples are shown in Fig. 3. The highly ordered mesoporous channel structure of pure SBA-15 can be observed in Fig. 3a, which shows a pore diameter of around 7-8 nm, in agreement with N_2 adsorption-desorption results. Due to the electronic density contrast of TEM, clear and gray stripes can be observed between empty channels and silica walls. When the SVO loading was increased to 51 wt% (Fig. 3b), the ordered array of mesopores remained intact. Silica walls remained white whereas the SVO particles, with a larger electronic density, turned black. The morphology results indicate that nanocrystalline SVO was inserted into the mesoporous channels of SBA-15 when urea was used as the chelating agent, which indicates a strong interaction between urea and metal ions that prevents the precipitation of silver and vanadium ions before the formation of silver vanadate-silica composites. EDX elemental analysis of a selected point of SBA-15 and the SBA-15 supported catalyst (Fig. 3) confirms the presence of SVO particles in the center of a SBA-15 channel.

3.4. DRIFTS study of adsorbed and photocatalytic oxidation of toluene

Fig. 4a shows the infrared spectra of toluene adsorbed at 300 K on fresh

SVO/SBA-15, SVO, and P25 (commercial TiO_2). For toluene adsorption, bands at 1635, 1606, 1496, 1447, and 1378 cm^{-1} were found, which correspond to the adsorption equilibrium of toluene on the samples at room temperature. The bands at 1606 and 1496 cm^{-1} can be assigned to the in-plane skeletal vibrations and the band at 1447 cm^{-1} corresponds to the vibrational mode of the C=C stretching bond of the aromatic ring [9]. The band at 1378 cm^{-1} is assigned to the symmetric CH_3 bending vibrations of adsorbed toluene [10]. As shown in Fig. 4a, the intensities of the bands for toluene adsorbed on SVO/SBA-15 are significantly higher than those for SVO and P25. Since the same amount of each sample was used for the DRIFTS experiments, SVO/SBA-15 adsorbed a much higher amount of toluene than did SVO and P25 at 300 K. Fig. 4b shows the IR spectra of the sample surfaces after 0.5 h of photocatalytic oxidation of toluene. For P25, after irradiating the adsorbed toluene with LED light, no significant formation of new surface species was observed. For the SVO/SBA-15 composites, however, new surface species formed. A shoulder near 1599 cm^{-1} is clearly visible and two weak bands at 1582 and 1452 cm^{-1} can be observed, which are the characteristic bands of benzaldehyde. In addition, MS analysis of the gaseous product indicates that traces of benzaldehyde, the only intermediate formed, were detected. Therefore, benzaldehyde is a potential intermediate of the photocatalytic oxidation of toluene in this study.

Table 2 shows the adsorption capacity and photocatalytic performance of various

samples. Before irradiation, the composites exhibit a much higher adsorption capability of toluene than those of plain SVO and P25. For the 17SVO/SBA-15 sample, the adsorption capacity is as high as 11.6 mg. When the silver vanadate content was increased to 51%, the adsorption capacity increased to 18.9 mg. The toluene adsorption capacity is thus affected by the silver vanadate content of SVO/SBA-15 composites. As shown in Table 2, all the SVO/SBA-15 samples have higher apparent rate constants than those of the bulk SVO and P25. In this study, the photocatalytic activity of the composite samples decreased in the order 51SVO/SBA-15 > 34SVO/SBA-15 > 17SVO/SBA-15. Generally speaking, the photocatalytic activity is strongly related to the crystalline phase. Konta et al. [11] reported that α-Ag$_3$VO$_4$ has stronger photocatalytic activity than those of β-AgVO$_3$ and Ag$_4$V$_2$O$_7$ for oxygen production from water-splitting under visible-light irradiation. However, the SVO/SBA-15 composites had the same crystalline phase as that of SVO; therefore, the crystalline phase is not the key factor influencing photoactivity.

3.5. DRIFTS study for regeneration test of photocatalyst

During the photocatalytic reaction, organic pollutants are supposed to be adsorbed and then degraded on the catalyst surface; therefore, it is important to evaluate the catalyst reliability in situ. Since 51SVO/SBA-15 had the highest apparent rate constant, it was chosen for the reliability test. A complete cycle was composed of adsorption under

darkness for 30 min and then an illumination reaction for 60 min. After the 1st cycle, the catalyst was regenerated in situ by further irradiating the LED light for 1 h. Then, the catalyst was reused in situ without any washing or thermal treatment for the 2nd cycle. The reliability test was stopped when the catalyst was deactivated as ascertained from DRIFTS and color analyses. The catalyst reliability results were expressed as IR spectra. The results of P25 and 51SVO/SBA-15 are shown in Fig. 5. After exposing P25 to LED light for 60 min, a decrease of the 1635, 1606, 1496, 1447, and 1378 cm^{-1} bands was observed, with new bands appearing at 1684 and 1582 cm^{-1} (Fig. 5a). This suggests that a fraction of the adsorbed toluene was photo-oxidized to benzaldehyde. The color of P25 became ocher after the 1st photocatalytic run. After the 2nd cycle, the intensities of the bands of toluene at dark adsorption for 30 min (Dark 2) were almost the same with those of illumination reaction for 60 min (VIS 2). Since the intensity of toluene was not reduced after illumination, the P25 had lost its photocatalytic activity. Several studies have observed TiO_2 deactivation during the photocatalytic oxidation of toluene [12-15]. Direct evidence comes from the color change of TiO_2 from white to yellow or yellow-brown after several hours of irradiation. It has been reported that the deactivation results from the accumulation of strongly adsorbed species, such as benzaldehyde and benzoic acid, on the TiO_2 surface [12-15]. However, deactivation does not occur for 51SVO/SBA-15. An obvious decrease of the toluene bands and an

intense appearance of the benzaldehyde bands were clearly observed for Dark 1 vs.VIS 1 (1st cycle) and Dark 2 vs. VIS 2 (2nd cycle), respectively (Fig. 5b). After 51SVO/SBA-15 was exposed to LED light for 1 h, it regenerated. The color of 51SVO/SBA-15 remained light orange color after the 2nd cycle. This proves that the 51SVO/SBA-15 photocatalyst is stable and can be regenerated and recycled without losing its original activity.

3.6. Roles of surface hydroxyl groups and surface acidity

It is well known that the adsorption capacity is mainly determined by the specific surface area and nature of the surface of the photocatalyst. Studies have shown that the much higher specific surface area and pore volume of TiO_2-containg mesoporous silica composites compared to those of pure titania are beneficial for the adsorption of organic pollutants [16-18]. In this study, the specific surface area of SVO/SBA-15 decreased with increasing amount of silver vanadate; however, the adsorption amount of toluene increased with increasing silver vanadate content of SVO/SBA-15. For SVO/SBA-15 composites, the toluene adsorption capacity is thus greatly influenced by the silver vanadate content, rather than the specific surface area. To further characterize the surface attributes that affect toluene adsorption, the high-frequency region of the IR spectra of the samples was examined using DRIFTS. Before DRIFTS measurements, the samples were dehydrated at 523 K. From the IR spectra, two broad strong bands,

ranging from 3700 to 3100 cm^{-1}, were observed for SVO/SBA-15 and SVO, whereas a

very weak band in the same range was observed for P25. The peaks in the range of

3700–3100 cm^{-1} may be due to the overlapping of various OH groups. For a quantitative

comparison of OH groups, the deconvolution of the peak was conducted using three

Gaussian curves based on the IR assignments of OH groups (at 3200, 3425, and 3687

cm^{-1}) reported in the literature. As shown in Table 2, the number of OH groups

decreased in the order 51SVO/SBA-15 > 34SVO/SBA-15 > 17SVO/SBA-15 > SVO >

P25, which agrees well with the rate constant results. Based on the proposed reaction

mechanism, during the photocatalysis reaction, the •OH radical species is generated via

the interaction of photogenerated holes, h^{+}, with surface hydroxyl groups [19]. These •

OH radicals can extract a hydrogen atom from the methyl groups of adsorbed toluene

molecules, the first step of the oxidative process, and then further produce benzaldehyde.

OH groups are considered strong Brønsted acid sites which provide more surface

adsorption centers for reactants. These groups inherited extraordinarily reactive

hydroxyl group radicals, which are capable of oxidizing the compounds adsorbed on

substrates. As a result, the photocatalytic process was accelerated. Moreover, the highly

polarized state of strong Brønsted acid sites produces effective hole-trapping centers,

thus limiting undesirable photo-carrier recombination. This tendency indicates that the

intensity of surface hydroxyl groups of the SVO/SBA-15 samples is a significant factor

that affects the photocatalytic activity.

To investigate the existence of Brønsted and Lewis acid sites, ammonia adsorption on the photocatalysts surface was studied. A literature survey indicates that IR spectroscopic studies of ammonia adsorbed on solid surfaces have made it possible to distinguish between Brønsted and Lewis acid sites of a catalyst [20-25]. Before the DRIFT measurements, the samples were saturated with NH_3/N_2, flushed with N_2 flow to remove physically adsorbed ammonia, and then heated from 303 K to 523 K. The intensity of chemisorption was determined based on the irreversible adsorption of ammonia. Fig. 6 shows the IR spectra of ammonia adsorbed onto SVO and SVO/SBA-15 samples which were heated at 523 K for 30 min. The existence of NH_4^+ ions adsorbed onto Brønsted acid sites of the silver vanadate surfaces is supported by the presence of a band at 1425 cm^{-1} due to the asymmetric deformation mode [20-22]. The band at 1604 cm^{-1} is assigned to NH_3 coordinately bonded to Lewis acid sites [23-25]. It can be concluded that both Brønsted and Lewis acid sites exist on the surfaces of SVO and SVO/SBA-15. The intensities of Brønsted and Lewis acid sites, detected at 1425 and 1604 cm^{-1}, respectively, follow the sequence: 51SVO/SBA-15 > 34SVO/SBA-15 > 17SVO/SBA-15 > SVO. The trend of Brønsted and Lewis acid sites is in agreement with that of the adsorption capacity. That is, higher intensities of Brønsted and Lewis acids of silver vanadate indicate a larger adsorption capacity for

toluene.

4. Conclusion

Environmentally friendly SVO/SBA-15 photocatalysts were synthesized using hydrothermal synthesis without a high-temperature calcination process. XRD and HRTEM results indicate that SVO/SBA-15 composites had the pure α-Ag_3VO_4 phase and that SVO dispersed well in the channels or on the surface of SBA-15 without affecting the SBA-15 mesoporous structure, respectively. The DRIFT spectra indicate that the main oxidation product of toluene is benzaldehyde, which is strongly adsorbed on the surface of the catalyst. The SVO/SBA-15 photocatalyst has a much higher photodegradation ability for toluene than does P25. Based on the stability test, the accumulation of benzaldehyde on the P25 surface appears to be responsible for its deactivation; no deactivation was observed for 51SVO/SBA-15, which was still stable after 2th cycle as evidenced by DRIFTS analysis. The existence of surface hydroxyl groups and the acidity of the SVO/SBA-15 composites was confirmed using DRIFTS The abundant surface hydroxyl groups and high intensities of Brønsted and Lewis acids are responsible for the enhanced adsorption capacity, superior photoactivity, and long term stability of SVO/SBA-15 composites.

References

[1]   K. Su, Z. Li, B. Cheng, K. Liao, D. Shen, Y. Wang, J. Mol. Catal. A 315 (2010) 60-68.

[2]   S. Zhang, D. Jiang, T. Tang, J. Li., Y. Xu, W. Shen, J. Xu, F. Deng, Catal. Today 158 (2010) 329-335.

[3]   T. Klimov, O. Gutierrez, L. Lizama, J. Amezcua, Micropor. Mesopor. Mater. 133 (2010) 91-99.

[4]   R. Zukerman, L. Vradman, L. Titelman, L. Zeiri, N. Perkas, A. Gedanken, M.V. Landau, M. Herskowitz, Mater. Chem. Phys. 122 (2010) 53-59.

[5]   K. Demeestere, J. Dewulf, H. Van Langenhove, Crit. Rev. Environ. Sci. Technol. 37 (2007) 489-538.

[6] H. Sun, J. Han, Y. Ding, W. Li, J. Duan, P. Chen, H. Lou, X. Zheng, Appl. Catal. A: Gen. 390 (2010) 26-34.

[7] C.M. Huang, G.T. Pan, Y.C.M. Li, M.H. Li, T.C.K. Yang, Appl. Catal. A: Gen. 358 (2009) 164-172.

[8] C.M. Huang, G.T. Pan, P.Y. Peng, T.C.K. Yang, J. Mol. Catal. A: Chem. 327 (2010) 38-44.

[9] M. Larrubia, G. Busca, Appl. Catal. B: Environ. 39 (2002) 343-352.

[10] M. Nagao, Y. Suda, Langmuir 5 (1989) 42-47.

[11] R. Konta, H. Kato, H. Kobayoshi, A. Kudo, Phys. Chem. Chem. Phys. 5 (2003) 3061-3065.

[12] G. Martra, S. Coluccia, L. Marchese, V. Augugliaro, V. Loddo, L. Palmisano, M. Schiavello, Catal. Today 53 (1999) 695-702.

[13] L. Cao, Z. Gao, S.L. Suib, T.N. Obee, S.O. Hay, J.D. Freihaut, J. Catal. 196 (2000) 253-261.

[14] M.C. Blount, J.L. Falconer, Appl. Catal. B: Environ. 39 (2002) 39-50.

[15] M. Lewandowski, D.F. Ollis, Appl. Catal. B: Environ. 43 (2003) 309-327.

[16] Y. Chen, Y. Huang, J. Xiu, X. Han, X. Bao, Appl. Catal. A: Gen. 273 (2004) 185-191.

[17] T. Hoshikawa, T. Ikebe, M. Yamada, R. Kikuchi, K. Eguchi, J. Photochem. Photobiol. A: Chem. 184 (2006) 78-85.

[18] J. Mo, Y. Zhang, Q. Xu, R. Yang, J. Hazard. Mater. 168 (2009) 276-281.

[19] V. Augugliaro, S. Coluccia, V. Loddo, L. Marchese, G. Martra, L. Palmisano, M. Schiavello, Appl. Catal. B: Environ. 20 (1999) 15-27.

[20] G. Ramis, L. Yi, G. Busca, Catal. Today 28 (1996) 373-380.

[21] M.A. Centeno, I. Carrizosa, J.A. Odriozola, Appl. Catal. B: Environ. 19 (1998)

67-73.

[22] L.C. Chen, G.T. Pan, T.C.K. Yang, T.W. Chung, C.M. Huang, J. Hazard. Mater.178

(2010) 644-651.

[23] J.R. Sohn, W.C. Park, Appl. Catal. A: Gen. 239 (2003) 269-278.

[24] J.R. Sohn, S.H. Lee, Appl. Catal. A: Gen. 266 (2004) 89-97.

[25] J.R. Sohn, J.S. Han, J. Ind. Eng. Chem. 11 (2005) 439-448.

Table Captions

Table 1 Specific surface areas, pore properties, and hydroxyl functional groups of P25,

SVO, SBA-15, and SVO/SBA-15.

Table 2 Adsorption capacities and apparent rate constants of P25, SVO, and

SVO/SBA-15 under 30 min of irradiation.

Table 1

Sample	S_{BET} (m^2g^{-1})	Pore volume (cm^3g^{-1})	Pore size (nm)
P25	56	0.25	17.52
SVO	2	0.002	7.30
SBA-15	787	1.09	7.61
17SVO/SBA-15	193	0.70	14.90
34SVO/SBA-15	141	0.54	16.14
51SVO/SBA-15	99	0.35	15.32

Table 2

Sample	Adsorption amount (mg)	Number of hydroxyl groups	Apparent rate constant (min^{-1})
P25	4.21	10.90	0.01
SVO	4.23	836.80	0.05
17SVO/SBA-15	11.56	3558.57	0.11
34SVO/SBA-15	17.59	5265.43	0.12
51SVO/SBA-15	18.95	6094.39	0.15

Figure Captions

Fig. 1   (a) Low-angle and (b) wide-angle XRD patterns of SVO and SVO/SBA-15.

Fig. 2 N_2 adsorption-desorption isotherms of SBA-15 and SVO/SBA-15 samples.

Fig. 3   HRTEM images of (a) SBA-15 and (b) 51SVO/SBA-15.

Fig. 4   DRIFTS spectra of samples (a) after adsorption of toluene for 30 min and (b)

after visible-light illumination for 30 min.

Fig. 5   DRIFT spectra of reliability test of (a) P25 and (b) 51SVO/SBA-15. VIS 1

denotes spectrum obtained under visible-light irradiation in the 1st cycle, and

VIS 2 denotes spectrum obtained under visible-light irradiation in the 2nd

cycle.

Fig. 6   IR spectra of NH_3 adsorbed onto SVO and SVO/SBA-15 samples at 523 K.

Figure 1 (a)
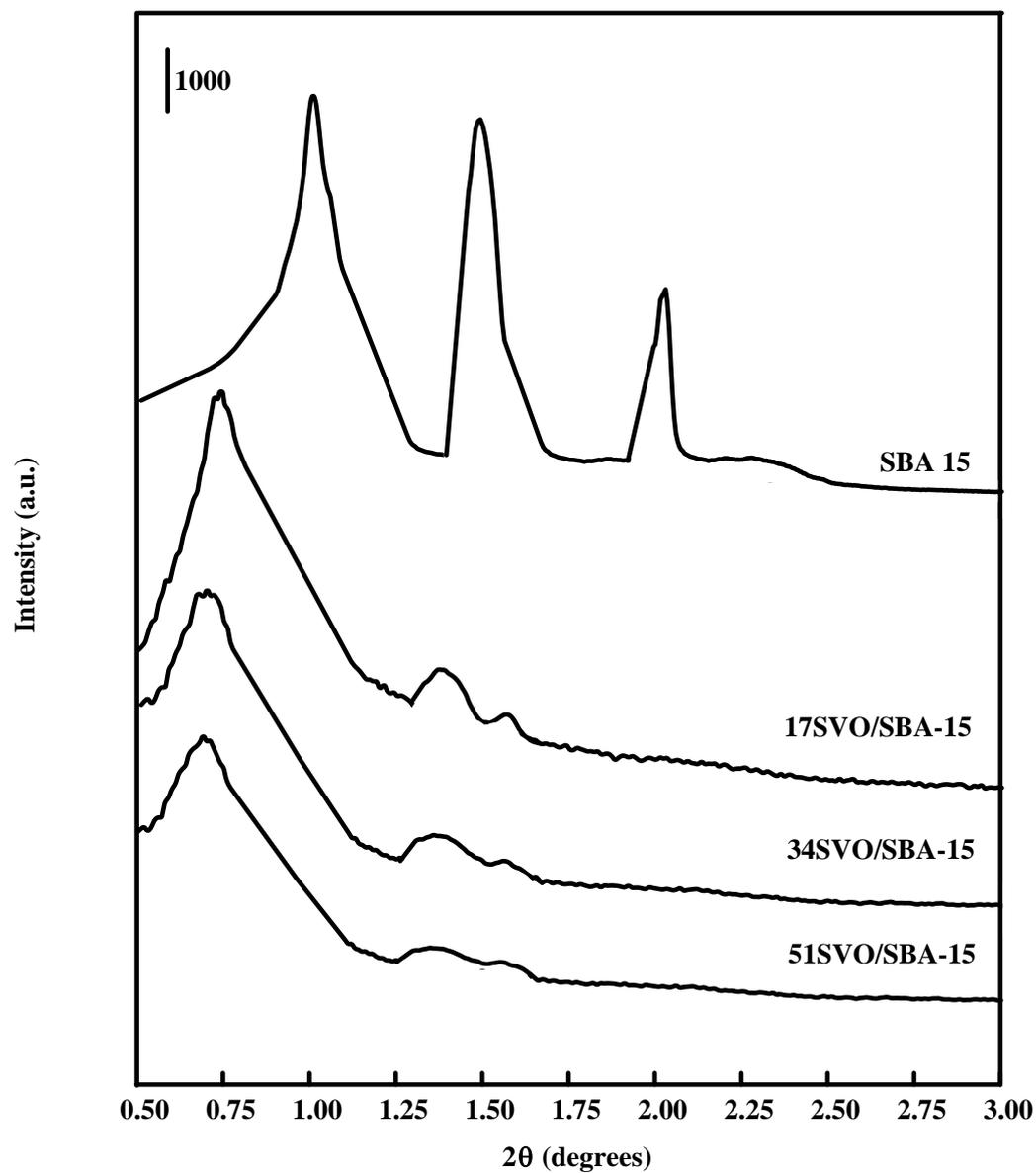
Figure 1 (b)
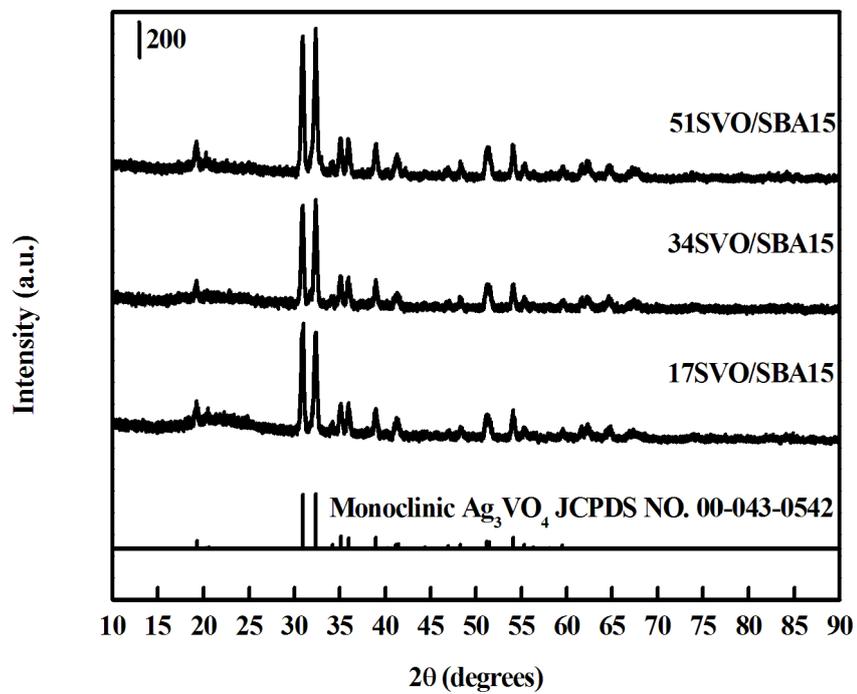
Figure 2
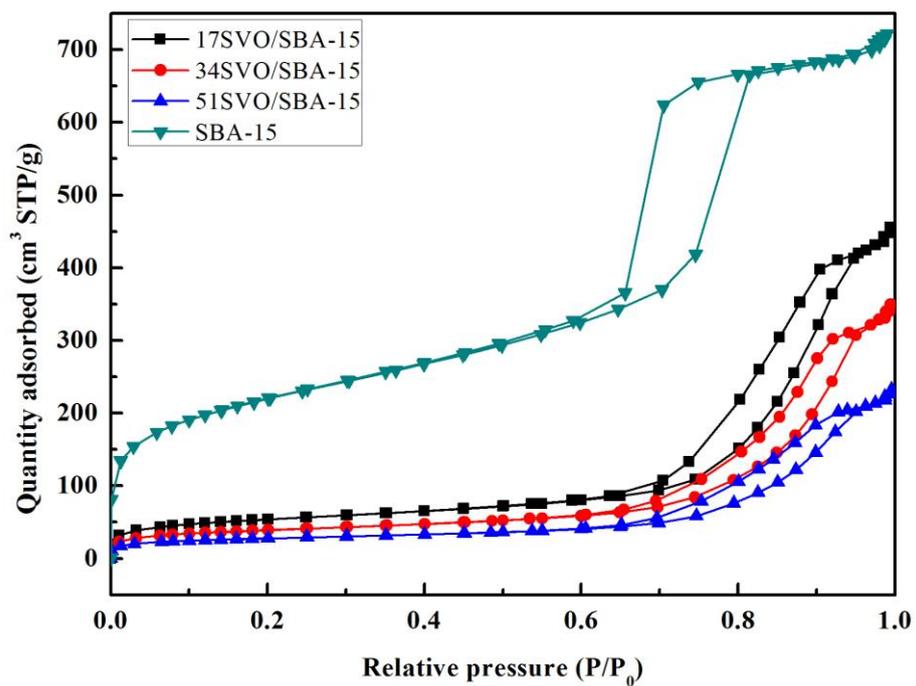
Figure 3 (a)
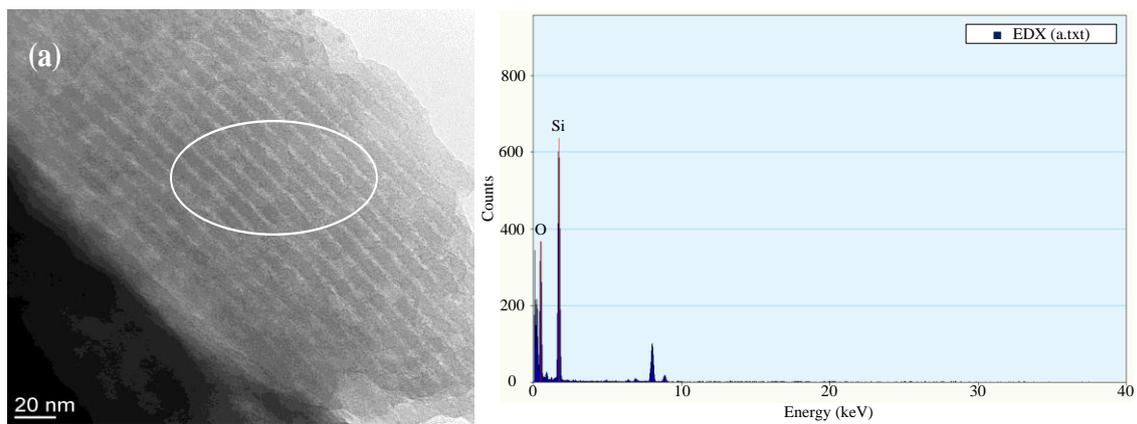
Figure 3 (b)
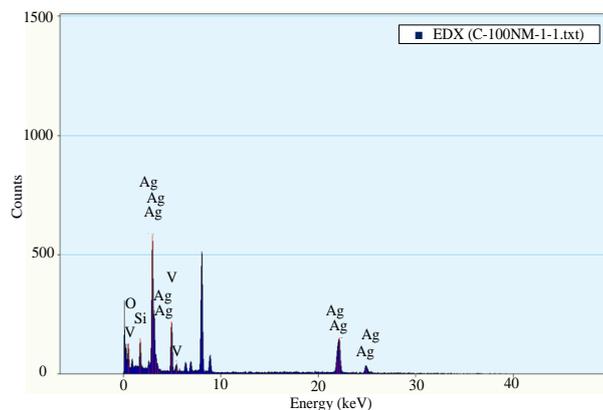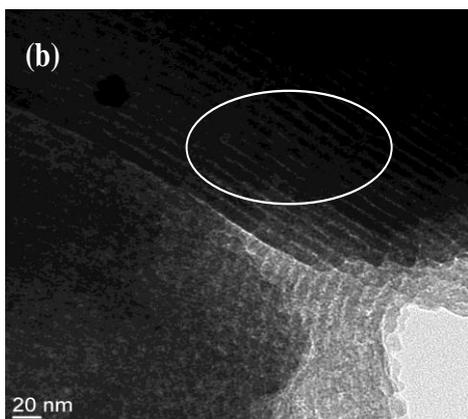
Figure 4 (a)
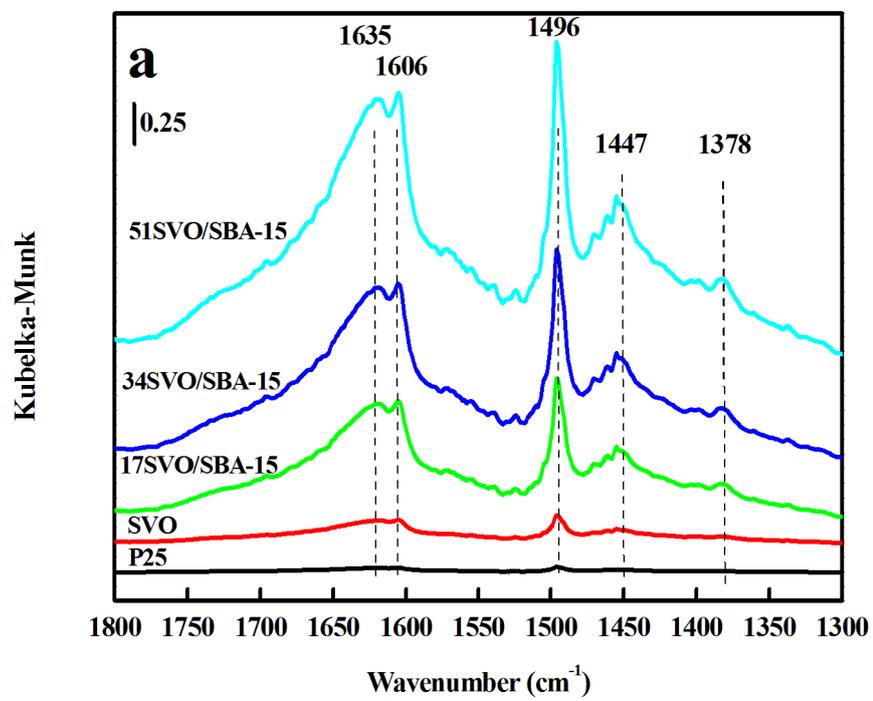
Figure 4 (b)
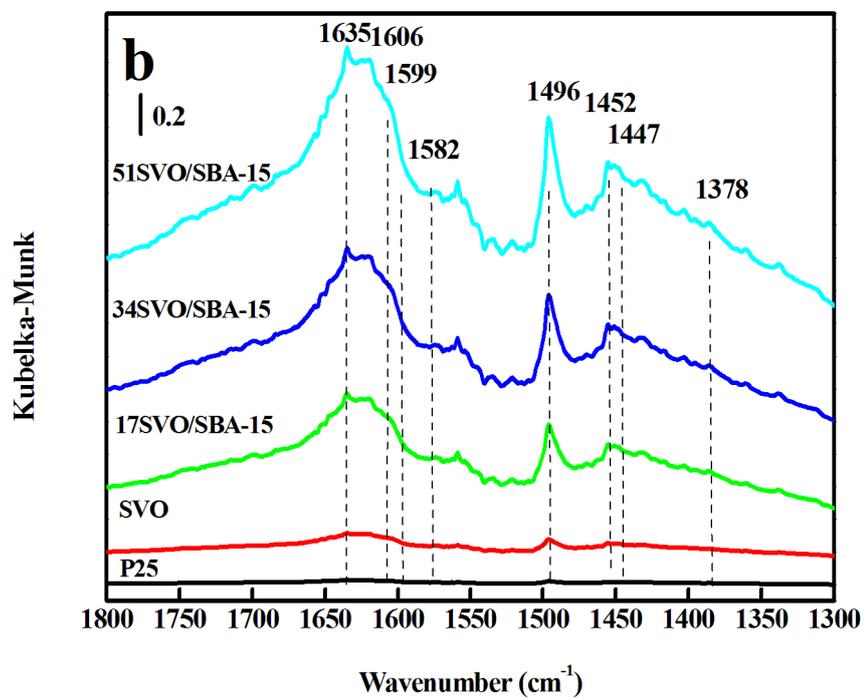
Figure 5 (a)

Figure 5 (b)

Figure 6